Bull. Chem. Soc. Ethiop. **2024**, 38(3), 751-763.
DOI: https://dx.doi.org/10.4314/bcse.v38i3.16

ISSN 1011-3924
Printed in Ethiopia
Online ISSN 1726-801X

HEPATOPROTECTIVE PERSPECTIVE OF NEWLY SYNTHESIZED 3-(3,5-BIS (TRI FLUORO METHYL) PHENYL)-5-METHYL-1-((1-METHYL-1H-PYRROL-2-YL) METHYL)-2-THIOXOIMIDAZOLIDIN-4-ONE AGAINST DIETHYL NITROSAMINE INDUCED LIVER INJURY IN RATS WITH MOLECULAR DOCKING INVESTIGATION

Lana S. Akree[1], Hiwa O. Ahmad[2,3] and Zahra A. Amin[1*]

[1]Clinical Analysis Department, College of Pharmacy, Hawler Medical University, Erbil, 44001, Iraq
[2]Pharmaceutical Chemistry Department, College of Pharmacy, Hawler Medical University, Erbil, 44001, Iraq
3Department of Pharmacy, College of Medicine, University of Kurdistan-Hawler, Erbil, 44001, Iraq

(Received November 30, 2023; Revised February 3, 2024; Accepted February 6, 2024)

ABSTRACT. The hepatoprotective effect of synthesized 3-(3,5-bis (trifluoromethyl) phenyl)-5-methyl-1-((1-methyl-1H-pyrrol-2-yl) methyl)-2-thioxoimidazolidin-4-one (3FL-M) was evaluated against diethyl nitrosamine-induced liver injury (DEN). Wistar rats were divided into 3 groups as: placebo (received 10% tween 80%), hepatotoxic control (injected with 200 mg/kg of DEN) and treatment (injected 200 mg/kg of DEN and received 50 mg/kg oral feeding of the synthesized 3FL-M). Half the number of the rats were sacrificed on 2nd week of the experiment, whereas the other half were sacrificed after 6 weeks. Blood was collected to run liver biochemical analysis, and to evaluate pro-inflammatory cytokines tumor necrosis factor-alpha TNF-α and interleukine6 IL-6. Liver sections were used to detect nuclear protein ki-67 and hepatocyte specific antibody HSA. 3FL-M was subjected to molecular docking calculations based on binding affinities towards TNF-α and IL-6. DEN-treated rats showed elevation in the liver serum enzymes as well as pro-inflammatory cytokines with clear destruction of the hepatic architecture, in contrast 3FL-M treated rats showed normalized liver enzymes and cytokines levels with resolution of the hepatocytes. Molecular modelling revealed that 3FL-M exhibited the significant affinities toward the binding pocket of the TNF-α and IL-6, however, further studies is recommended for developing it as a chemotherapeutic drug-like molecule.

KEY WORDS: DEN, Hepatoprotective, TNF-α, IL-6, Molecular docking

INTRODUCTION

Liver cancer is a well-known and serious type of malignancy that has accelerated growth and bad prognosis. Liver cancer can start as liver injury, such as fibrosis and progress to cirrhosis and ends up in carcinoma [1]. Liver cancer is a cause of high morbidity and mortality rates worldwide, because of its difficult diagnosis and prolonged asymptomatic stage [2]. The liver is largest organ in the human body, and it is in-charge of many vital biochemical activities, most importantly the detoxification of the internal and external waste materials and metabolic waste, and has a big role in the immune defence [3]. There is a relation between the increased incidences of liver cancer and viral liver infections in developed and developing countries [4]. Nitrosamines, are well established toxic chemical compounds that are known for causing different types of malignancies in humans and experimental animals [5]. 2-Thioxoimidazolidin-4-one ring (2-thiohydantoin) has been extensively studied and present in a wide range of biological active compound with a variety of substituents at positions of 1,3, and 5 [6, 7]. Structure activity relationship (SAR) revealed that thioxoimidazolidin-4-one (X = S) derivatives were 10-fold more active than corresponding hydantoin derivatives (X = O) [8].

*Corresponding author. E-mail: zahraa.alnajaar@hmu.edu.krd

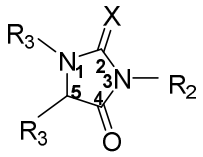

a) X = O
b) X = S

Scheme 1. General structure of rhodanine (X = S) and 2,4-thiazolidinediones (X = O). R groups mark positions of their potential functionalization.

The aim of this study is to evaluate the protective effects of a novel chemical derivative 3FL-M on liver injury induced by DEN in experimental rats.

EXPERIMENTAL

Chemical techniques

Infra-red spectra (IR). The range 4000-600 cm^{-1} were used to record the infra-red spectra by a SHIMADZU CORP series FTIR machine. Samples were either one of powder or thin films. Each absorption was estimated in cm^{-1}.

Nuclear magnetic resonance (NMR). ^{1}H-NMR and ^{13}C-NMR spectra were recorded on a Bruker DPX 400 (400 MHz) or DPX 500 (500 MHz) spectrometer. Chemical shifts were stated as parts per million (ppm) directed from tetramethyl silane (the internal standard). NMR spectrum was documented in solutions in deuterated-dimethyl sulfoxide (DMSO-d6) or chloroform ($CDCl_3$). HMBC and HSQC experiments were used on the same spectrometers to confirm assignments when necessary.

Mass spectrometry (LCMS). Experiments were performed using a Waters 2790 liquid chromatography system and a Waters ZQ mass spectrometer. Samples were loaded using a Gilson 232XL auto-sampler. Data of low-resolution spectroscopy were detected by Fisons VG Platform II quadrupole machine using electrospray ionization, however; data of high-resolution mass spectrometric was determined in electrospray (ES) mode on a Waters Q-TOF micro-mass spectrometer.

Method

General procedure

A mixture of CH_2Cl_2 (10 mL) and trimethylamine were used to dissolve amino acid methyl ester HCl Aldehyde and sodium triacetoxyborohydride were added to the solutions and stirred at room temperature (*ca*. 20 °C). 1-isothiocyanato-3,5-bis (trifluoromethyl) benzene was added to the mixture and continued to stir for another 1 hour. The organic phase evaporated under reduced pressure and 3x10 mL of hexane was added to the solid to extract all impurities. The product was dried by high vacuum and records the NMR spectroscopy [9].

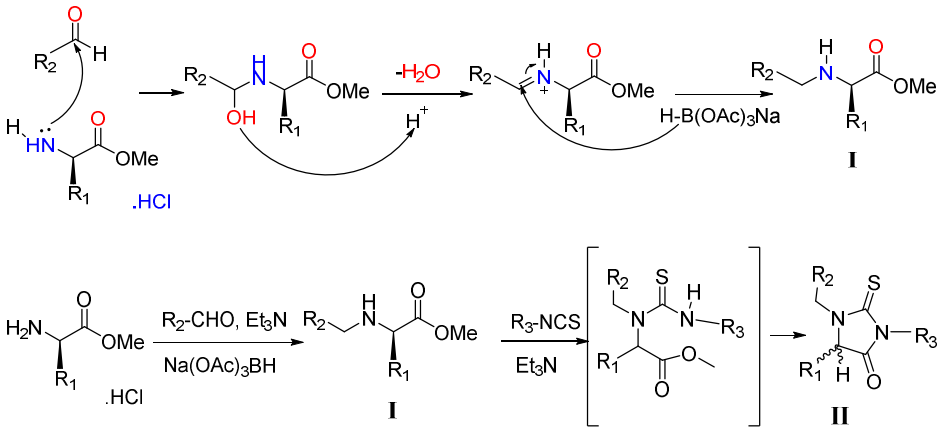

Scheme 2. I: The reduction process of imine to form corresponding amine. II: Synthesis of racemic tri-substituted 2-thiohydantoin [10].

DEN model of hepatotoxicity

In this study, twenty-four male rats weighing (250-280 g) were used. The study was performed at the animal house laboratory of College of Pharmacy-Hawler Medical University under the authorization of the ethics committee of College of Pharmacy (no. HMU.PH.EC/205). Rats were maintained with standard food and water and kept at (23 ± 4°C) with 12h–12h light/dark cycle under 50-60% humidity conditions. Experimental rat groups (n = 8) were allocated as: Group I (placebo group) administered orally with 10% of Tween. Group II (hepatotoxic control) administered with single dose of 200 mg/kg DEN [11] by intraperitoneal injection. Group III (Treatment group) administered with single dose of 200 mg/kg DEN by intraperitoneal injection and administered orally with 50 mg/kg of 3FL-M. The oral feedings were given twice a day for 15 days. Half number of the rats in each group was sacrificed at day 15 whereas the other half was euthanized after 6 weeks. Blood sera were collected for analysing liver function test and pro-inflammatory cytokines interlukin-6 (IL-6) and tumor necrosis factor alpha (TNFα) by ELISA method. Liver tissues were fixed in 10% formalin then sectioned, processed, and stained with hematoxylin and eosin (H&E) stains and nuclear protein (Ki-67) and hepatocyte specific antibody (HSA) were detected by immunohistochemistry technique.

Molecular docking

The two-dimensional (2-D) structure of the 3FL-M molecule (Figure 1) was built using Chemdraw professional 16.0 and converted to 3-dimensional (3-D) structures using Chem3D 16.0 module and saved as a pdb format structures (http://www.cambridgesoft.com/). Geister charges and hydrogen were added to the ligand and AutoDock Tools 1.5.7 software was used to convert file to the pdbqt format. Then, to do the docking stimulation, the ligand molecule was fed as input into AutoDock Vina (https://vina.scripps.edu/). Target of necrosis factor TNF-α (PDB ID:1TNF) and Human interleukin-6 IL-6 (PDB ID: 1IL6) X-ray crystal structures were obtained from the RCSB Protein Data Bank web server (http://www.rcsb.org/pdb/). The active binding sites were identified using Discovery Studio visualizer 2021. The grid dimensions were set at 17.9x 53.3x 38.5 (PDB ID: 1TNF), and 3.5 x --3.5 x 0.4 (PDB ID: 1IL6) according to the coordinates x, y, and z, for the target active binding sites identified in Discovery Studio visualizer 2021. Polar

hydrogen and Kollman charges were added, and the water molecules were removed from the receptors. The pdbqt format of the receptors were created by AutoDock Tools 1.5.7. AutoDock Vina was compiled and runs under Windows 10.0 Professional operating system. Discovery Studio 2021 was used to deduce the visual manner of the interaction between the ligands and the target protein.

The binding affinity (*K*i) of 3FL-M for selected targets were calculated using Eq. 1

$$Ki = e^{(\Delta G\ /(Rx\ t))} \quad (1)$$

where ΔG is the binding energy in kcal/mol, the universal gas constant R = 1.987 kcal/K/mol, at room temperature (25 °C) T = 273 + 25 = 298 K. *K*i is the inhibition constant where the Ki principally depends on the binding (or association) constant (Kb) having a unit of mM [12].

ADME prediction

Prediction of pharmacokinetics and physicochemical parameters plays a key role in drug design [13]. The evaluation of drug-likeness properties was evaluated for 3FL-M molecule using SwissADME (http://www.swissadme.ch/), (https://biosig.lab.uq.edu.au/pkcsm/prediction) and admetSAR (http://lmmd.ecust.edu.cn/admetsar2) [14]. Drug-like molecules must obey Lipinski's rule of five (RO5) as follows: the molecular weight MW of the active oral drug should be ≤500 Da; the log P should be <5; the number of hydrogen bond acceptors should be ≤ 10; the number of hydrogen bond donors should be ≤ 5; and the number of rotatable bonds should be ≤10 [15].

Statistical analysis

The data were expressed as Mean ± SEM of different groups. The differences between the mean values were evaluated by two-way analysis of variance (ANOVA) with Post-hoc Bonferroni test. A value of $p < 0.05$ was considered as significant. Analysis was conducted by using the SPSS-28, Graphpad-8.4.2 and Excel-2019 programs.

RESULTS AND DISCUSSION

Synthesis of 3FL-M

L-Alanine methyl ester hydrochloride salt (1.00 g, 7.16 mmol) was dissolved in dichloromethane (16 mL) in the presence of triethylamine (0.93 mL, 6.3 mmol). 1-Methyl-1H-pyrrole-2-carbaldehyde (0.80 mL, 7.40 mmol) and sodium triacetoxyborohydride (2.1 g, 9.91 mmol) were added and the mixture, allowing stirring over night at room temperature. 1-Isothiocyanato-3,5-bis (trifluoromethyl) benzene (2.60 mL, 14.23 mmol) and triethylamine (0.20 mL, 1.43 mmol) were added, and the mixture was stirred for another hour (Scheme 3).

Yield = 64.0%, m.p. 173-174 °C, HRMS calculated for $C_{18}H_{15}F_6N_3OS$ m/z $[EI]^+$ 435.0840; found 435.0840; ^{1}H-NMR (500 MHz, $CDCl_3$): δ 7.86 (s, 1H, C**H**CF_3), δ 7.79 (s, 2H, C**H**CC**H**), δ 6.61 (t, *J* = 3.2 Hz, 1H, C**H**NCH_3), δ 6.16 (dd, *J* = 3.5, 1.7 Hz, 1H, C**H**CHNCH_3), δ 6.04 (t, *J* = 3.2 Hz, 1H, C**H**CNCH_3), δ 5.69 (d, *J* = 15.6 Hz, 1H, C$\mathbf{H}_A$CH_BN), δ 4.49 (d, *J* = 15.6 Hz, 1H, CH_AC$\mathbf{H}_B$N), δ 3.98 (q, *J* = 7.2 Hz, 1H, C**H**CH_3), δ 3.60 (s, 3H, N**C**$\mathbf{H}_3$), δ 1.51 (d, *J* = 7.2 Hz, 3H, CHC$\mathbf{H}_3$), ^{13}C-NMR (126 MHz, $CDCl_3$): δ 179.3 (**C**=S), δ 172.5 (**C**O), δ 134.3 (**C**NCH_3), δ 132.2 (**C**HN), δ 124.3 (2x**C**HN), δ 124.2 (**C**HCCF_3), δ 122.7 (**C**HCHN), δ 121.7 (**C**HCN), δ 111.3 (2 x **C**CF_3), δ 107.7 (2 x **C**F_3), δ 57.2 (**C**HCH_3), δ 40.8 (N**C**H_3), δ 34.8 (**C**H_2NCH_3), δ 15.5 (CH**C**$\mathbf{H}_3$). IR (neat): ν_{max} = 1756 cm^{-1} (C=O), 1480 cm^{-1} (C=S).

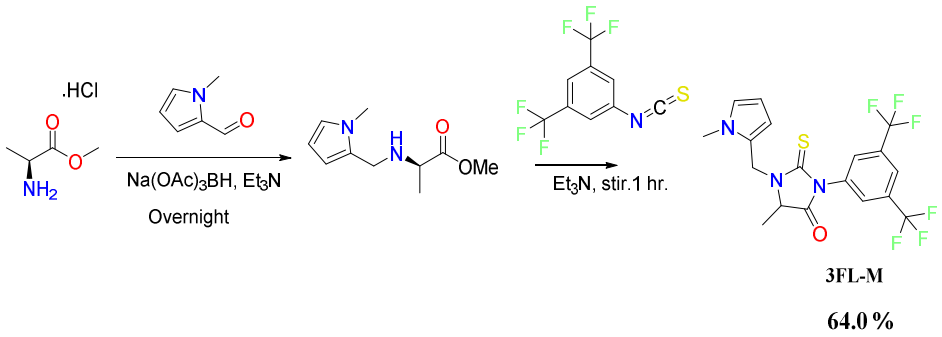

Scheme 3. Synthesis of 3-(3,5-bis(trifluoromethyl)phenyl)-5-methyl-1-((1-methyl-1H-pyrrol-2-yl) methyl)-2-thioxoimidazolidin-4-one (3FL-M).

3FL-M protective effect against diethyl nitrosamine induced liver injury

After six weeks of diethyl nitrosamine injection to the rat's, a significant increase was observed in the liver function enzymes: aspartate aminotransferase (AST), alanine aminotransferase (ALT), alkaline phosphatase (ALP) which are the most sensitive indicators of liver injury when compared with the placebo or vehicle group (Table 1), whereas the treatment with 3FL-M produced significant restoration of these enzymes to their normal levels.

Table 1. Effect of the synthesized (3FL-M) on liver function parameters.

Groups	AST (U/L)	ALT (U/L)	ALP (U/L)
At week 2			
P	78.1±0.1 *	61.1±0.2 *	131.1±0.1 *
DEN	173.3±0.1 #	177.1±0.4 #	289.3±0.9 #
3FL-M	81.5±0.2*#	76.6±2.1*#	145.4±0.2*#
At week 6			
P	80.2±0.2 *	60.4±0.22 *	125.5±0.5 *
DEN	300.1±0.2#	280.1±0.1#	400.4±0.3#
3FL-M	82.0±0.1*	62.00±0.9*	122.2±0.2*

The values are expressed as the mean ± SEM; P = placebo; DEN = diethyl nitrosamine; 3FL-M treated group; AST = aspartate aminotransferase; ALT = alanine aminotransferase; ALP = alkaline phosphatase. $p < 0.05$ (*) indicates significance difference when compared to DEN group while (#) indicates significance difference when compared to P group.

Likewise, significant increase in the proinflammatory cytokines (TNF-α and IL-6) was documented in rat group treated with diethyl nitrosamine and remarkably decrease of the same cytokines in 3FL-M treated rats (Figure 1).

Liver tissue sections showed variable histological changes between placebo and DEN; however, treatment with 3FL-M (2 week and 6 weeks) lead to obvious hepatic upgrading characterized as no or very little signs of fibrosis, less infiltration of inflammatory cells, decreased levels of dilation of bile canaliculi and sinusoids and regularity of liver structure (Figure 2 A and D). Immunohistochemical staining of HSA and Ki67 proteins were consistent with the haematoxylin and eosin-stained sections for both durations of treatments as negative or few positive cells were observed. (Figure 2B, E and C, F), respectively.

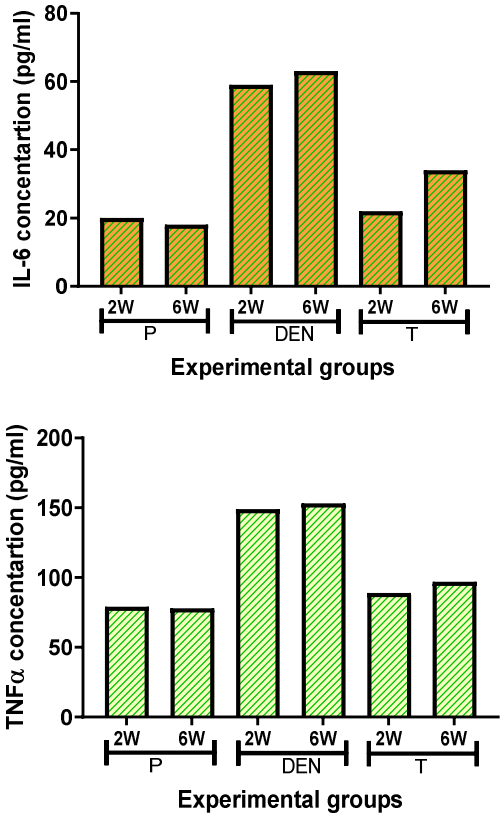

Figure 1. Effect of synthesized 3FL-M on proinflammatory cytokines IL-6 and TNF-α; P: Placebo, DEN: diethyl nitrosamine and T: treatment group.

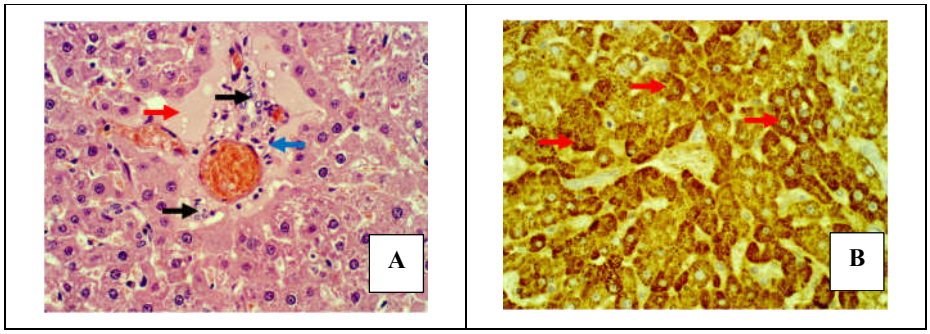

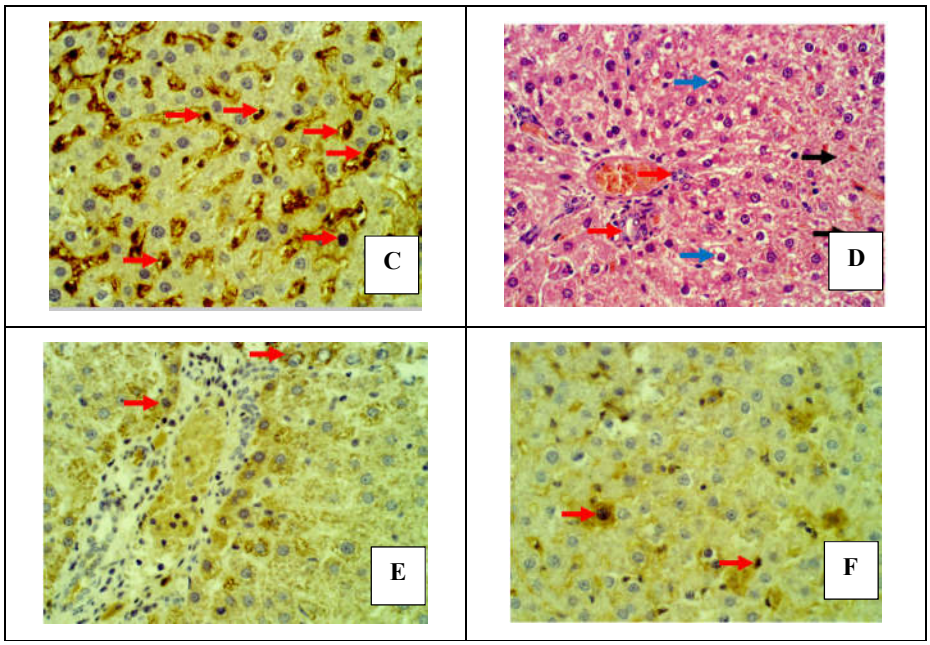

Figure 2. Effect of synthesized 3FL-M on liver architecture. (A) two weeks 3FL-M treated group showed hyperplasia bile cuniculi (black arrow), infiltration of mononuclear inflammatory cells (blue arrow), deposition of eosinophilic material as indicator of fibrosis (red arrow). *Section stained with H&E. 400x.* (B) two weeks 3FL-M treated group showed strong positive staining with *HSA* antibodies in the cytoplasm of hepatocytes as golden-brown granules (red arrow). *IHC Section stained with HSA-ab 400x.* (C) two weeks 3FL-M treated group showed positively staining nucleus of hepatocytes with *Ki67* antibodies (red arrow). *IHC Section stained with Ki67-ab 400x.* (D) Six weeks 3FL-M treated group showed necrosis in the affected hepatocytes (black arrow), vacuolar degeneration in others (blue arrow), hyperplasia of bile cuniculi (red arrow). *Section stained with H and E. 400x.* (E) Six weeks 3FL-M treated group showed few weakly positive staining with *HSA* antibodies in the cytoplasm of hepatocytes as golden-brown granules around portal area (red arrow). *IHC Section stained with HSA - ab 400x*. (F) Six weeks 3FL-M treated group showed few positively staining nuclei of hepatocytes with *Ki67* antibodies (red arrow).

Section stained with Ki67-ab 400x

Synthesized compound has been investigated for its binding site efficacies to the receptors involved in the liver injury including tumour necrosis factor α (TNFα) and interleukin-6 (IL-6) (Table 2) [16, 17].

3FL-M showed selective binding energies of (-9.0 and -7.8 kcal/mol) toward TNF-α (PDB ID: 1TNF) and IL-6 (PDB ID: 1IL6), respectively. Five hydrogen bonds formed with active site residues of TNF-α (PDB ID: 1TNF) including GLU B: 116, GLU A: 116, GLU C: 116, PRO A: 100, and GLN A: 102. One of the hydrogen bonds occurred between GLN A: 102 and C=S. The remaining carbon hydrogen bonds are between GLU B: 116, GLU A: 116, GLU C: 116, and PRO A: 100. Other than the hydrogen bonding, one pi-anion and two alkyl bonds interaction were

observed between five membered rings of 1-methyl-1H-pyrrole and alkyl flouro-substituted, respectively. The remaining nine halogen bonds are between active site residues of GLU C: 101, GLN B: 102, PRO C: 100, GLN C: 102, ARG C: 103, and GLU A: 104 with halogen (flour) at trifluoromethyl substitueted on phenyl ring (Figure 3). The active site of IL-6 (PDB ID: 1IL6) consisted mainly of SER A: 177, ALA A: 69, PHE A: 174, PHE A: 75, MET A: 68, ALA A: 69, PRO-A: 66, LEU A: 65, LEU A: 166, GLU A: 173, GLU A: 173, and MET A: 68. Fluorine groups at methyl substitueted on phenyl ring formed three hydrogen bonds with SER A: 177, ALA A: 69, and PHE A: 174. Five membered rings of 1-methyl-1H-pyrrole and alkyl flouro-substituted interacted with PRO A: 66, LEU A: 65, LEU A: 166, and PHE A: 75, MET A: 68, ALA A: 69, respectively. Furthermore, the halogens (flour) formed two halogen bonds with GLU A: 173 and MET A: 68 (Figure 4).

Table 2. In silico molecular docking results of 3FL-M interaction with tumour necrosis factor α (TNFα) and interleukin-6 (IL-6).

Name	Binding energy (kcal/mol)	Predicted inhibition constant p*Ki* (μM)	Interaction position	Distance Å	Bonding type
TNF-α (PDB ID:1TNF)	-9.0	6.7	GLU B: 116	5.85	Carbon-hydrogen bond
			GLU A: 116	3.54	
			GLU C: 116	3.38	
			PRO A: 100	3.33	
			GLN A:102	3.37	Conventional-hydrogen bond
			CYS C: 101	3.91	Alkyl
			CYS C: 69	4.28	Alkyl
			GLU C: 101	2.75	Halogen
			GLN B: 102	2.87	
			PRO C: 100	2.77	
			GLN C: 102	3.21	
			ARG C: 103	3.59	
			GLU A: 104	3.17	
IL-6 (PDB ID: 1IL6)	-7.8	6.2	SER A: 177	2.40	Conventional - hydrogen bond
			ALA A:69	2.33	Carbon-hydrogen bond
			PHE A:174	2.61	
			PHE A:75	5.16	Pi-alkyl
			MET A: 68	4.20	
			ALA A: 69	4.27	
			PRO A: 66	4.62	
			LEU A:65	4.94	
			LEU A: 166	4.63	
			GLU A:173	4.20	Pi-anion
			GLU A: 173	3.29, 3.85	Halogen
			MET A: 68	3.61	

ADMET analysis

The ADMET study is among the most essential parts of computational drug design. ADMET was estimated for all synthesized compounds using an online web server, i.e. SwissADME (http://www.swissadme.ch/), (https://biosig.lab.uq.edu.au/pkcsm/prediction) and admetSAR (http://lmmd.ecust.edu.cn/admetsar2).[18] The obtained ADMET properties are presented in detail in Table 3.

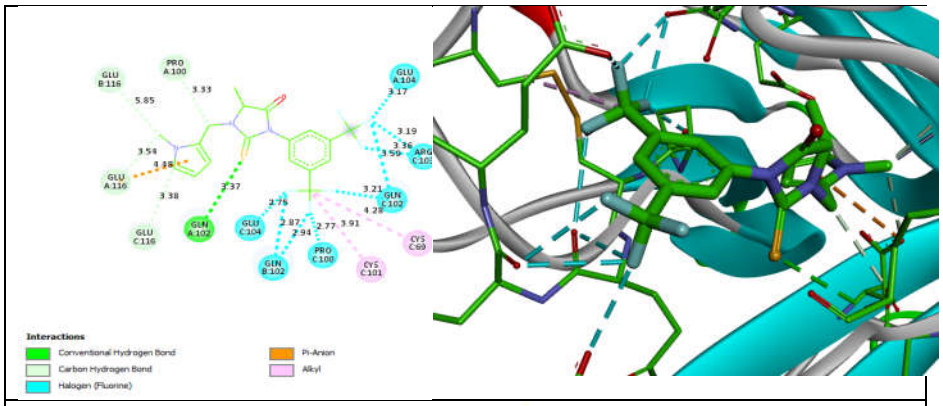

Figure 3. 2D and 3D representation of the interaction of 3FL-M with TNF-α (PDB ID: 1TNF).

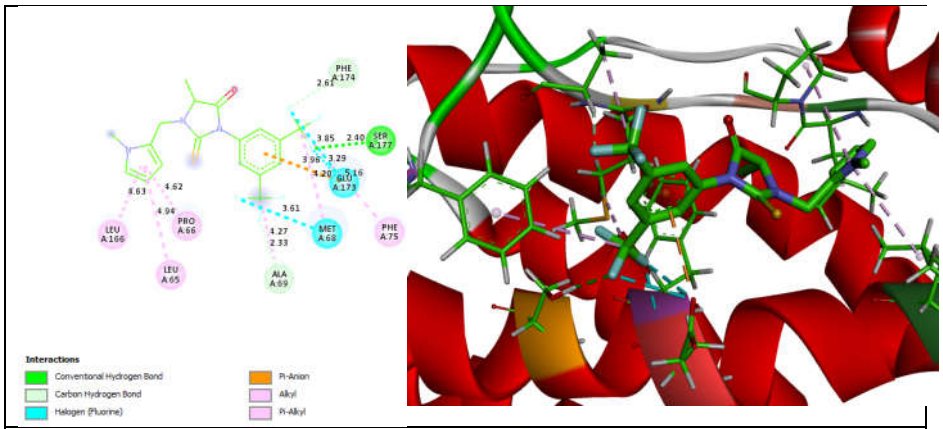

Figure 4. 2D and 3D representation of the interaction of 3FL-M with IL-6 (PDB ID: 1IL6).

Table 3. List of ADME and physicochemical properties of 5B2T.

#	MW (g/mol)	BBB+	Caco2+	HIA+	Logp	TPSA A2	H-bond don.	H-bond acc.	RBs	Skin permeability
	180–500	180–500	180–500	180–500	<5	≤140	≤ 5	≤ 10	≤10	> -2.5 Low skin permeability
3FL-M	435.39	0.9500	118.7	90.136	4.58	60.57	0	7	5	-2.804
	MW: Molecular Weight; BBB+: Blood-Brain Barrier; Caco2+, Caco-2: Permeability; HIA+: %human intestinal absorption; logp: logarithm of partition coefficient between n-octanol and water; TPSA2: topological polar surface area; H-bond acc.: number of hydrogen bond acceptors; H-bond don.: number of hydrogen bond donors; RBs: number of rotatable bond.									

Synthesized 3FL-M exhibits acceptable ADMET molecular weight properties of 435.35 (g/mol). A significant value of 95% revealed a high chance of crossing blood brain barrier. The percentage of human intestinal drug absorption 90.136% was in the acceptable range (> 80). Octanol–water partition coefficient (Log P) of 4.58 was found to be less than 5 with no more than

one violation is allowed. The topological surface areas (TPSA) were found to be in the acceptable range (< 140). In addition, H-bond acceptors (HBA) and donors (HBD) were found to be ≤ 10, and ≤ 5, respectively.

Thiohydantoin has five potential substituent sites, including two hydrogen bond donors and two hydrogen bond acceptors [19]. 2-Thiohydantoins and their analogues are among the anticancer agents that are presented as clinical candidates for treating different cancer types. Trisubstituted 2-thiohydantoin derivative named enzalutamide was used as a possible treatment generate potent androgen receptor antagonists [20]. In medicinal chemistry, the addition of halogen atoms to a candidate chemical to enhance its biological profile has recently emerged as a key drug development method, and it is frequently used in analogue-based drug discovery. Moreover, 35% of the top 15 best-selling drugs between 2010 and 2016 were halogenated including "blockbuster drugs" [21]. Halogen bonds have the effect of stabilizing intra- and intermolecular interactions, which can stabilize ligand interactions and impact molecular folding [22]. Based on the previous study, alkyle substituents on C-5 position has a little influence on activity. This information has an agreement with our previous study indicated that 5-benzylidene-2-thiohydantoin has lower binding site energies toward TNF-α (PDB ID: 1TNF) and IL-6 (PDB ID: 1IL6), respectively [23]. Tri flouro methyl group was maintained at the meta position of phenyl at N-2 of both 3FL-M. previous results showed that the incorporation of lipophilic linker at positions N1 and N2 with flouro substituted at phenyl ring improved β-selectivity and potency [24]. A trifluoromethyl analogue of celecoxib has been found to suppress pro-inflammatory cytokine and possibility of directly suppressed neutrophil activation, while celecoxib significantly increases the production of IL-6. TFM-C suppresses the production of inflammatory cytokines from macrophages and the activation of mast cells as well as the subsequent recruitment of leukocytes (Figure 5) [25].

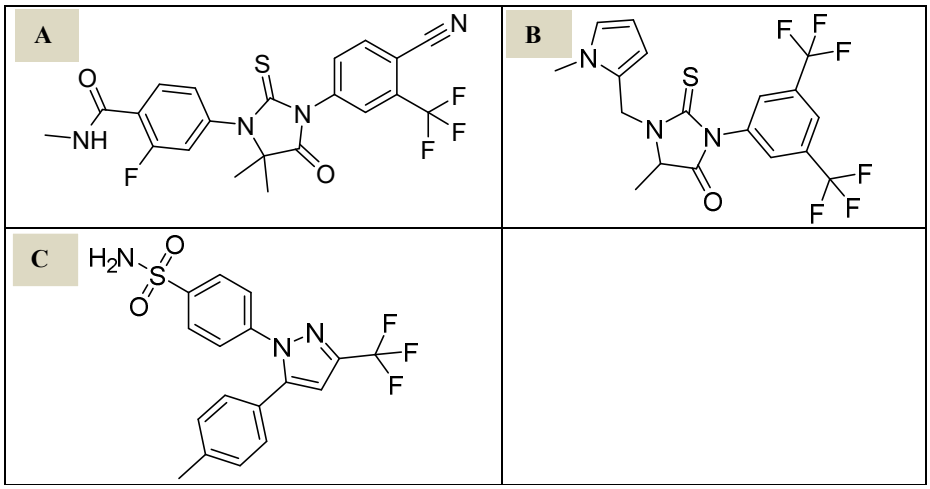

Figure 5. 2-D structures of A: enzalutamide, B: 3FL-M, C: A trifluoromethyl analogue of celecoxib.

Diethyl nitrosamine (DEN) is a well-established toxic and carcinogenic substance that is known for initiating various types of cancer including liver cancer in experimental rats. The administration of DEN for prolonged periods of time is proved to cause liver tumors. A single intraperitoneal injection of DEN is shown to cause irreversible liver injury in experimental animal

model (200 mg/kg) [26]. The high ability of the DEN to produce reactive oxygen species (ROS) is the main factor that enables this substance to initiate toxicity and eventually cancer, this can result in the damaging of DNA, lipids, and proteins by oxidative stress. For establishing the previously mentioned actions, DEN must be first metabolized by enzyme cytochrome p450, this enables the DEN to release high ROS causing DNA-adducts by alkylation and lipid peroxidation of cell membrane leading eventually in cell death. The administration of DEN cause 100% successful induction of liver tumors in experimental animals [27]. In the present study, a single intraperitoneal injection of 200 mg/kg of DEN was performed to the experimental rats to initiate liver injury for the purpose of experimenting the protective activities of the synthesized 3FL-M in resolving liver injury. The biochemical test results in Table 1 is showing obvious elevation in the biochemical parameters (including ALT-AST-ALP) in the DEN-treated rats that indicates liver injury. The cytoplasmic release of these parameters to the blood after the rupture of the cell membrane induced by DEN may be attributed to the elevation of these markers [28]. In contrast, in the 3FL-M treated rats, there was a massive decline in the biochemical markers, the same results which were found in a study of the effects of synthesized 5B2T on liver injury induced by DEN [23]. The assumed capability of the 3FL-M to inhibit the progression of the hepatic injury is attributed to its ability in conserving the integrity of the cell's membrane as a result inhibiting the leakage of the important enzymes from the cell to the outer environment. The present study also included the elevation of two important pro-inflammatory cytokines in the serum, these are TNF-α and IL-6 by ELISA technique. Figure 1 illustrates the effects of the synthesized 3FL-M as a treatment on the levels of the pro-inflammatory cytokines TNF-α and IL-6 in serum by using the ELISA technique. In the DEN-treated rats' group, there was a high elevation in the levels of the serum cytokines, indicating the development of strong liver injury in this group (inflammation). However, the rats of the 3FL-M-treated group showed a massive decline in the levels of the same cytokines if compared to the previous group, suggesting the efficiency of the substance as a liver protective agent. The previous finding is further supported histopathologically and immuno-histochemically. After the administration of DEN, the hepatic architecture was disorganized and lost. This a results of a serious of oxidation reactions, which lead eventually to the transformation of the normal liver cell into a neoplastic cell [29]. Figure 2 showing the histopathological and immuno-histochemical findings. Liver sections of the 3FL-M-treated rats tested histopathologically of the two weeks duration revealed infiltration of inflammatory cells and fibrosis. On the other hand, the results of the 6 weeks 3FL-M-treated rats showed necrosis in the affected hepatocytes. The 2 weeks stained 3FL-M-treated hepatic sections with HSA immuno-histochemically showed strong positive staining with HSA antibodies as golden-brown cytoplasmic granules. In contrast the 6 weeks 3FL-M-treated hepatic sections showed few weakly positive staining with HSA antibodies in the cytoplasm of the affected hepatocytes. Two weeks 3FL-M-treated hepatic sections stained with ki-67 antibodies immuno-histochemically showed strong positive staining of the nucleus of the affected hepatocytes with ki-67 antibodies, in contrast to the 6 weeks treated sections that revealed few positive staining of the nuclease of the liver cells with ki-67 antibodies. In a research performed on the elevation of ki-67 antibodies in DEN-induced hepatocellular carcinoma in experimental rats, here was a massive increase I the number of the positively stained cells with ki-67 following the DEN administration [30]. Considering the molecular docking studies, the synthesized 3FL-M illustrated attractive results as treatment theses were represented by improvements in the prognosis of the liver injury, this highlights the possibility of implicating this substance as a real and crucial treatment for various liver disorders.

CONCLUSION

In the presented study, we described the synthesis of 3-(3,5-bis (trifluoromethyl)phenyl)-5-methyl-1-((1-methyl-1H-pyrrol-2-yl)methyl)-2-thioxoimidazolidin-4-one. Synthesized compound was examined in vivo against diethyl nitrosamine induced liver injury. Furthermore,

molecular docking study revealed that 3FL-M has potential binding site affinity toward the pro-inflammatory cytokines TNF-α and IL-6 receptors, suggesting that tri substituted-2-thioxoimidazolidin-4-one (2-thiohydantoin) derivatives could be considered for the development of effective anti-inflammatory agents. Further study is needed to use an extra dose of oral administration to exhibit anti-tumer activity of tri substituted-2-thioxoimidazolidin-4-one (2-thiohydantoin) derivatives.

REFERENCES

1. Antunes, C.; Arbo, M.; Konrath, E. Hepatoprotective native plants documented in Brazilian traditional medicine literature: Current knowledge and prospects. *Chem. Biod.* **2022**, 19, 6.
2. Huang, A.; Yang, X.; Chung, W.; Dennison, R.; Zhou, J. Targeted therapy for hepatocellular carcinoma. *Sig. Trans. Targ. Ther.* **2020**, 5, 146.
3. Fang, Y.; Tian, S.; Pan, Y.; Wang, Y.; Tang, T.; Yu, X.; Wu, Y.; Shi, M. Pyroptosis: A new frontier in cancer. *Biomed. Pharm.* **2020**, 121, 109595.
4. Lavanchy, D. Evolving epidemiology of hepatitis C virus. *Clin. Micro. Inf.* **2011**, 17, 107-115.
5. Fahmi, A.; Hassanen, M.; Abdur-Rahman, E. Phytochemicals, antioxidant activity and hepatoprotective effect of ginger (*Zingiber officinale*) on diethylnitrosamine toxicity in rats. *Biomarkers* **2019**, 24, 436-447.
6. Elhady, H.; El-Sayed, R.; Al-Nathali, H. Design, synthesis and evaluation of anticancer activity of novel 2-thioxoimidazolidin-4-one derivatives bearing pyrazole, triazole and benzoxazole moieties. *Chem. Cen. J.* **2018**, 12, 1-13.
7. Alosaimi, A.; Saad, H.; Al-Hazmi, H.; Refat, M. In situ acetonitrile/water mixed solvents: An ecofriendly synthesis and structure Explanations of Cu(II), Co(II), and Ni(II) complexes of thioxoimidazolidine. *Bull. Chem. Soc. Ethiop.* **2021**, 35, 351-364.
8. Tejchman, W.; Orwat, B.; Korona-Głowniak, I.; Barbasz, A.; Kownacki, I.; Latacz, G.; Handzlik, J.; Żesławska, E.; Malm, A. Highly efficient microwave synthesis of rhodanine and 2-thiohydantoin derivatives and determination of relationships between their chemical structures and antibacterial activity. *RSC Adv.* **2019**, 9, 39367-39380.
9. Ahmad, H.O. Kinetics and mechanism of racemisation reactions of configurationally labile stereogenic centres in drug-like molecules in aqueous solutions; thiohydantoins and related compounds, *PhD Thesis*, Cardiff University; **2015**.
10. Sim, M.; Ganesan, A. Solution-phase synthesis of a combinatorial thiohydantoin library1. *J. Org. Chem.* **1997**, 62, 3230-3235.
11. Rezaie, A.; Pashmforosh, M.; Karamallah, H.; Fazlara, A.; Haghighat, A.; Shahriari, A. Hepatoprotective effect of caffeine on diethylnitrosamine-induced liver injury in rats. *Bulg. J. Vet. Med.* **2014**, 17, 3.
12. Ashraf, S.; Elkhalifa, O.; Mehmood, K.; Adnan, M.; Khan, N.; Eltoum, A.; Baig, M. Multi-targeted molecular docking, pharmacokinetics, and drug-likeness evaluation of okra-derived ligand abscisic acid targeting signaling proteins involved in the development of diabetes. *Molecules* **2021**, 26, 5957.
13. Rahman, A.; Majid, N.; Abd Wahid, M.; Ismail, H.; Tap, F.; Zainudin, A.; Zainol, S.; Mohammad, M. Molecular docking analysis and anti-hyperglycaemic activity of Synacinn in streptozotocin-induced rats. *RSC adv.* **2020**, 10, 34581-34594.
14. Daina, A.; Michielin, O.; Zoete, V. Swiss ADME: A free web tool to evaluate pharmacokinetics, drug-likeness and medicinal chemistry friendliness of small molecules. *Sci. Rep.* **2017**, 7, 1-13.
15. Lipinski, C.; Lombardo, F.; Dominy, F.; Feeney; P. Experimental and computational approaches to esutimate solubility and permeability in drug discovery and development settings. *Adv. Drug. Deliv. Rev.* **2012**, 64, 4-17.

16. Dong, Y.; Liu, Y.; Kou, X.; Jing, Y.; Sun, K.; Sheng, D.; Yu, G.; Yu, D.; Zhao, Q.; Zhao, X. The protective or damaging effect of tumor necrosis factor-α in acute liver injury is concentration-dependent. *Chem. Biosci.* **2016**, 6, 1-10.
17. Schmidt-Arras, D.; Rose-John, S. IL-6 pathway in the liver: from physiopathology to therapy. *J. Hepatol.* **2016**, 64, 1403-1415.
18. Ameen, R.; Amin, Z.; Ahmad, H.; Ghafur, D.; Toma, M.; Sabah, N.; Fakhir, M.; Abdulla, G. Gastroprotective effect of rhodanine and 2,4-thiazolidinediones scaffolds in rat stomachs by contribution of anti-apoptotic (BCL-2) and tumor suppressor (P53) proteins. *Sci. Rep.* **2024**, 14, 1699.
19. Faghihi, K.; Valikhani, N. New polyamides based on 1,3-bis (4-carboxy phenoxy) propane and hydantoin derivatives: synthesis and properties. *Bull. Chem. Soc.Ethiop.* **2010**, 24, 77-83.
20. Cho, S.; Kim, S.; Shin, D. Recent applications of hydantoin and thiohydantoin in medicinal chemistry. *Eur. J. Med. Chem.* **2019**, 164, 517-545.
21. Suárez-Castro, A.; Valle-Sánchez, M.; Cortés-García, C.; Chacón-García, L. Molecular docking in halogen bonding. *Molecular Docking*. **2018**, DOI: 10.5772/intechopen.72994
22. Gilday, L.; Robinson, S.; Barendt, T.; Langton, M.; Mullaney, B.; Beer, B. Halogen bonding in supramolecular chemistry. *Chem. Rev.* **2015**, 115, 7118-7195.
23. Akree, L.; Amin, Z.; Ahmad, H. In silico and in vivo hepatoprotective activity of the synthesized 5-benzylidene-2-thiohydantoin against diethylnitrosamine-induced liver injury in a rat model. *Sci. Rep.* **2023**, 13, 4681.
24. Khirallah, S.; Ramadan, H.; Shawky, A.; Qahl, S.; Baty, R.; Alqadri, N.; Alsuhaibani, A.; Jaremko, A.; Emwas, H.; Saied, E. Development of novel 1, 3-disubstituted-2-thiohydantoin analogues with potent anti-inflammatory activity; in vitro and in silico assessments. *Molecules* **2022**, 27, 6271.
25. Chiba, A.; Mizuno, M.; Tomi, C.; Tajima, R.; Alloza, R.; Di Penta,A.; Yamamura, T.; Vandenbroeck, K.; Miyake, S. A 4-trifluoromethyl analogue of celecoxib inhibits arthritis by suppressing innate immune cell activation. *Arthr. Res. Ther.* **2012**, 14, 1-10.
26. Bishayee, A.; Bhatia, D.; Thoppil, R.; Darvesh, A.; Nevo, E.; Lansky, E. Pomegranate-mediated chemoprevention of experimental hepatocarcinogenesis involves Nrf2-regulated antioxidant mechanisms. *Carcinogen.* **2011**, 32, 888-896.
27. Gupta, P.; Bhatia, N.; Bansal, M.; Koul, A. Lycopene modulates cellular proliferation, glycolysis and hepatic ultrastructure during hepatocellular carcinoma. *World J. Hep.* **2016**, 8, 1222.
28. Wu, S.; Lin, Y.; Ye, Y.; Xiong, X.; Li, F.; Cheng, F. Prognostic value of alkaline phosphatase, gamma-glutamyl transpeptidase and lactate dehydrogenase in hepatocellular carcinoma patients treated with liver resection. *Int. J. Sur.* **2016**, 36, 143-151.
29. Kahrilas, G.; Blotevogel, J.; Stewart, P.; Borch, T. Biocides in hydraulic fracturing fluids: A critical review of their usage, mobility, degradation, and toxicity. *Environ. Sci. Technol.* **2015**, 49, 16-32.
30. Youssef, M.; Maghraby, H.; Youssef, E.; El Sayed, M. Expression of Ki 67 in hepatocellular carcinoma induced by diethylnitrosamine in mice and its correlation with histopathological alterations. *J. Appl. Pharm. Sci.* **2012**, 2, 52-59.